



# Cold Spray Construction of Nanostructured Titania Coatings for Photocatalytic Applications

Jin Liu<sup>1,2</sup> · Yi Liu<sup>1,2</sup> · Xinkun Suo<sup>2</sup> · Leszek Latka<sup>3</sup> · Aleksandra Małachowski<sup>3</sup> · Deping Lu<sup>1</sup> · Hua Li<sup>2</sup>

Submitted: 9 October 2020 / in revised form: 11 January 2021 / Accepted: 12 January 2021 / Published online: 27 January 2021  
© ASM International 2021

**Abstract** Nano-titania (TiO<sub>2</sub>) has drawn considerable attention for decades for its excellent photocatalytic activity. The use of photocatalyst TiO<sub>2</sub> in the form of surface coating is usually desired for long-term recyclable photocatalytic performances. Yet deposition of the coatings with appropriate nanostructures persists challenging. Thermal spray processing usually triggered loss of photocatalytic anatase in the coatings. To retain anatase structure from starting TiO<sub>2</sub> powder, in this study, cold spray was employed to deposit TiO<sub>2</sub> nanostructured coatings using TiO<sub>2</sub> nanoparticles as the starting feedstock. The mechanically blended Al-7.5 wt.% TiO<sub>2</sub> powder was used as the feedstock for the coating fabrication, and Al was

used as the binder for the nano-TiO<sub>2</sub> particles. The coatings containing anatase phase were successfully fabricated and showed good long-term recyclable performance and service life. After methylene blue degradation testing for three times, the photocatalytic efficiency of the coatings still remained over 90% of the initial photocatalytic efficiency. After high-pressure gas purge and flame sweep processing, the coatings retained the initial nanostructures at their surfaces. The cold spray technical route might open a new window for making the coatings of temperature-sensitive nanosized particles for functional applications.

**Keywords** anatase · cold spray · nanoparticles · photocatalytic performances · TiO<sub>2</sub> · TiO<sub>2</sub>-Al composites

This article is an invited paper selected from presentations at the 10th Asian Thermal Spray Conference (ATSC 2020) and has been expanded from the original presentation. ATSC 2020 was held in Ningbo, China, from November 1–3, 2020, and was organized by the Asian Thermal Spray Society with Ningbo Institute of Materials Technology and Engineering, Chinese Academy of Sciences as the Host Organizer.

✉ Jin Liu  
ljustb@163.com

✉ Hua Li  
lihua@nimte.ac.cn

<sup>1</sup> Institute of Applied Physics, Jiangxi Engineering Laboratory of Metal Surface Strengthening Technology, Jiangxi Academy of Sciences, Nanchang 300029, China

<sup>2</sup> Zhejiang Engineering Research Center for Biomedical Materials, Cixi Institute of Biomedical Engineering, Ningbo Institute of Materials Technology and Engineering, Chinese Academy of Sciences, Ningbo 315201, China

<sup>3</sup> Faculty of Mechanics, Wrocław University of Science and Technology, WUTS, ul. Lukasiewicza 5, 50-370 Wrocław, Poland

## Introduction

Nanosized titanium dioxide (TiO<sub>2</sub>) is known as a photocatalyst and antibacterial agent with high chemical stability, good durability, and cost efficiency. It can convert light energy into chemical energy to accomplish strong oxidizing ability, effectively degrading various organic and inorganic pollutants in air and water. Consequently, TiO<sub>2</sub> has been widely used in air purification, antibacterial treatment, textile industry, household appliances, automobile industry, and national defense and military fields (Ref 1-3). Nanosized anatase powder, which has large specific surface area and strong photocatalytic activity, is an ideal photocatalyst and active oxygen antibacterial agent (Ref 4). However, in practical applications, due to the extremely small size of nano-TiO<sub>2</sub>, the particles usually easily agglomerate, resulting in decreased specific surface area, and consequently subsided photocatalytic activity and antibacterial performance. In addition, direct use of nano-

TiO<sub>2</sub> particles makes recycling difficult and may cause secondary pollution (Ref 5, 6). The powder particles in nanosizes alone are toxic, and they have been labelled as carcinogenic by inhalation as their aerodynamic diameter is less than 10 microns. Deposition of nano-TiO<sub>2</sub> particles on the surfaces of devices, components, etc., to form firmly adhered functional coating offered the benefit of reusability and non-pollution (Ref 7, 8). Many attempts have been made to fabricate TiO<sub>2</sub> coatings using a variety of techniques such as sol-gel (Ref 9), self-assembly (Ref 10), spray pyrolysis (Ref 11), magnetron sputtering (Ref 12) and thermal spray (Ref 2, 13, 14). The processing approaches like sol-gel, self-assembly and spray pyrolysis are complicated and have environmental concerns, and the magnetron sputtering method is usually associated with expensive equipment, high production cost, and difficulties in depositing large-area coatings. In contrast, thermal spray technique has the advantages of low cost, ease of large-scale coating fabrication; it is therefore a good candidate for making coatings of a vast variety of materials. There have been inspiring pioneering efforts in depositing nano-titania coatings through thermal spray processing (Ref 15, 16). However, as the heating temperature is above 600 °C, anatase starts to transform into rutile structure with reduced photocatalytic activity. Since the typical thermal spray processes rely on melting of powder, for instance the plasma jet temperature during plasma-spray reaches above 20,000 K, and the flame temperature during HVOF-spray reaches about 3000 K, it keeps challenging to retain the anatase phase during the typical thermal spray coating deposition. Besides, sintering of the TiO<sub>2</sub> particles would occur during high-temperature processing, giving rise to a reduction in specific surface area. Both effects would deteriorate the photocatalytic performances of the TiO<sub>2</sub> coating. Therefore, alternatively, for thermal spray fabrication of nano-titania coatings, suspension or precursor was usually employed, which has shown capability to alleviate the heating of the nanoparticles during the spraying (Ref 2, 17). Yet the poor adhesion and cohesion of the coatings remain as the major hurdle affecting their long-term functional applications.

Cold spray has been rapidly developed in recent years as an additive manufacturing technique that uses high-speed gas flow to accelerate solid particles, so that the particles hit a preset substrate at a very high speed to cause plastic deformation to form a coating (Ref 18). Inspiring research has been extensively carried out for cold spraying metallic materials (Ref 19) and even ceramics (Ref 4). It would be exciting if nano-titania could be cold-sprayed to make coating, since by doing so, both the nanosizes and anatase structure of titania can be effectively retained after the spraying. Research efforts have been made on cold spray deposition of nanostructured ceramic powder for functional

applications, in particular nanostructured titania powder (Ref 20–27). These coatings, however, do not possess desired photocatalytic activities, for their structures are not optimal. Due to the extremely small sizes, directly depositing the particles in nanosizes by traditional cold spray keeps challenging. Alternatively, vacuum cold spray has been attempted to make the nano-titania coatings (Ref 28). In that case, nanosized powder can be successfully deposited to form nanostructured coatings, regardless of the necessity of further improving adhesion/cohesion of the coatings. In this work, we tried to tackle the problems of coating fabrication of nano-titania for desired photocatalytic performances. To accomplish this, aluminum was used as metallic binder to host the nanoparticles in the coatings.

## Materials and Methods

7.5 wt.% commercial granulated nano-TiO<sub>2</sub> powder (P25, containing anatase phase (76.6 vol.%) and rutile phase (23.4 vol.%) and 92.5 wt.% spherical aluminum powder (– 200+400 mesh, Tianjiu, Changsha, China) were mixed at room temperature using alcohol as the medium. The starting Al-TiO<sub>2</sub> powder feedstock for the cold spraying was prepared through the drying processing using a vacuum drying oven. The substrate was Al 7075 (Al alloy) pretreated with sandblasting. A custom built cold spray system was employed for the spraying. This system is similar to the commercial cold spray systems, and the stainless steel nozzle had the throat diameter of 3 mm, the exit diameter of 10 mm, and the length of 225 mm. For the spraying, nitrogen was used as the propulsive gas with the pressure of 2.5 MPa and the temperature of 350 °C. The powder feedrate was 50 g/min. The stand-off distance and traverse speed of the gun were set as 30 mm and 300 mm/s, respectively.

X-ray diffraction (Bruker AXS D8) using Cu K $\alpha$  radiation was employed to characterize the crystal structure of the feedstock powder and cold sprayed coatings. The volume percentage of anatase (*A*) was determined according to the following formula (Ref 29):

$$A = \frac{1}{1 + 1.265 \frac{I_R}{I_A}} \times 100\% \quad (\text{Eq 1})$$

where *I<sub>A</sub>* and *I<sub>R</sub>* are the x-ray intensities of the (101) peak of anatase and the (110) peak of rutile, respectively. Integrated intensities of the three main XRD peaks for each phase were used for the calculation. Scanning electron microscope (SEM, FEI Sirion200, USA) was used to analyze the surface morphology of the Al-TiO<sub>2</sub> coatings, as well as their cross-sectional morphology (etched by

15 wt.% NaOH aqueous solution). Qualitative analyses of the elements Ti, Al and O within the coatings were carried out using the EDS (Oxford AZtec X-Max 20, UK). Cold field-emission scanning electron microscope (FESEM, Hitachi S-4800, Japan) was also employed to characterize the topographical microstructure of the as-sprayed coatings.

Photocatalytic activity of the coatings was evaluated by measuring the degradation of methylene blue (MB, Aladdin Reagent Corp., China) under irradiation of high-pressure mercury ultraviolet lamp of 365 nm wavelength and 500 watts power (GGZ500). For the testing, the 10 mm × 10 mm sample was immersed in a double-walled beaker which was positioned 20 cm below the lamp and was equipped with controllable circulating cooling water to keep room temperature in order to eliminate thermal effect. The sample was placed in 30 mL of MB solution, and the MB solution was continuously stirred with a magnetic stir bar. The whole testing system was subject to dark environment for 0.5 h to achieve an adsorption/desorption equilibrium prior to photo-irradiation. The light absorption plate reader (Molecular Devices SpectraMax 190, USA) was used to measure the absorption intensity with the absorption characteristic wavelength of 664 nm. The degradation rate was calculated by the formula:

$$D_t = \frac{C_0 - C_t}{C_0} \times 100\% \quad (\text{Eq 2})$$

where  $C_0$  and  $C_t$  are the initial concentration and the reaction time concentration of the MB, respectively,  $D_t$  is the degradation rate at the corresponding time point. The UV radiation testing for each sample was repeated for three consecutive times.

## Results and Discussion

The morphologies of the starting  $\text{TiO}_2$  and the Al- $\text{TiO}_2$  powder feedstock used in this work are shown in Fig. 1. The  $\text{TiO}_2$  particles show an average particle size of about 25 nm (Fig. 1a). After the pretreatment of mixing-stirring-drying, the Al- $\text{TiO}_2$  composite particles show a spherical shape, taking the spherical Al particle as the core, and it is enveloped by a thick layer of the nano- $\text{TiO}_2$  particles (Fig. 1b, c and d). These nano- $\text{TiO}_2$  particles were fixed on the surface of the micron-sized spherical Al particle during the pretreatment processing of mixing-stirring-drying.

XRD patterns of the Al- $\text{TiO}_2$  feedstock powder and the cold sprayed coatings are shown in Fig. 2. The feedstock powder and the coatings are both mainly composed of Al and  $\text{TiO}_2$ , demonstrating that the nano- $\text{TiO}_2$  particles were successfully deposited, coexisting with the aluminum matrix. In the feedstock powder and the coatings,  $\text{TiO}_2$  has

two crystal structures: anatase phase and rutile phase. According to the calculation result based on the XRD patterns using the formula (1), for the Al- $\text{TiO}_2$  feedstock powder, the volume fraction of the anatase phase over the total of  $\text{TiO}_2$  is 76.6%, while for the Al- $\text{TiO}_2$  coatings, the volume fraction of the anatase phase over the total of  $\text{TiO}_2$  is 74.1%. It indicates that the phase composition of  $\text{TiO}_2$  particles has no remarkable change during the cold spray processing, and the anatase phase retained its crystal structure. The peak referring to  $\text{Al}_2\text{O}_3$  phase appeared for the cold sprayed coatings, likely due to the slight oxidation of Al during the cold spraying or due to the embedded grit since alumina was used as the blasting media.

Surface microstructures of the Al- $\text{TiO}_2$  coatings are shown in Fig. 3. The surface of the coatings is like undulating hills (Fig. 3a), which is typical feature of common cold sprayed coatings. The undulating surface topography is caused by the plastic deformation of the Al matrix during the deposition. It is surprisingly noted that the surface of the coatings is tightly and evenly covered by a thick layer of nano- $\text{TiO}_2$  particles, and no cracks and other defects are seen (Fig. 3b). During the cold spraying, there is a bow wave in front of the plate, which obstructs the movement of nanoparticles and hindered their deposition (Ref 4). That theory explained the reason why nanoparticles cannot be deposited by conventional cold spray. In this work, as the nano- $\text{TiO}_2$  particles are designed to tightly adhere to the micron-sized Al particles, the bow wave slightly affects the movement of large micron-sized Al- $\text{TiO}_2$  composite particles, so the nano- $\text{TiO}_2$  particles can be deposited relatively easily.

Cross-sectional morphologies of the Al- $\text{TiO}_2$  coatings are shown in Fig. 4. The thickness of the Al- $\text{TiO}_2$  coatings ranges from 20 to 50  $\mu\text{m}$ , and the coatings adhered to the substrate tightly with no notable cracks (Fig. 4a). Comparing with the nano- $\text{TiO}_2$  coatings deposited by other techniques (Ref 29-31) with a thickness of up to 3 micron, the thickness of the cold sprayed coating has been significantly increased. Magnified views of the coating (Fig. 4b) indicate that the forming process of the Al- $\text{TiO}_2$  coating is similar as those reported for cold sprayed metallic coatings. The presence of nano- $\text{TiO}_2$  particles did not bring about remarkable difficulties in cold spray deposition of the Al-based materials. The pits on the upper surface of the substrate imply its recessed and activated state as achieved by the impingement of the Al- $\text{TiO}_2$  composite particles. Significant plastic deformation was clearly seen for the Al matrix, which is essential for bonding of the materials onto the substrate upon the impingement. The accumulation of deformed Al also gave rise to adhesion of the nano- $\text{TiO}_2$  particles, which are located in between adjacent Al particles (Fig. 4b).

**Fig. 1** SEM morphology of the starting TiO<sub>2</sub> (a) and Al-TiO<sub>2</sub> powder (b) used in this work, (c, d) high-resolution topographical images of the Al-TiO<sub>2</sub> particles showing adherence of nano-TiO<sub>2</sub> particles on Al matrix

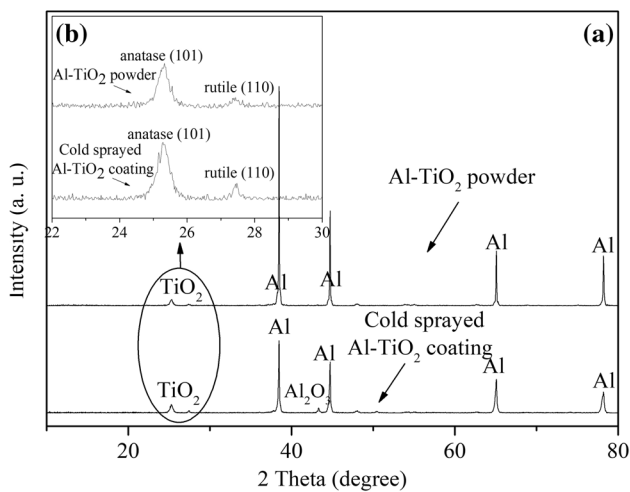
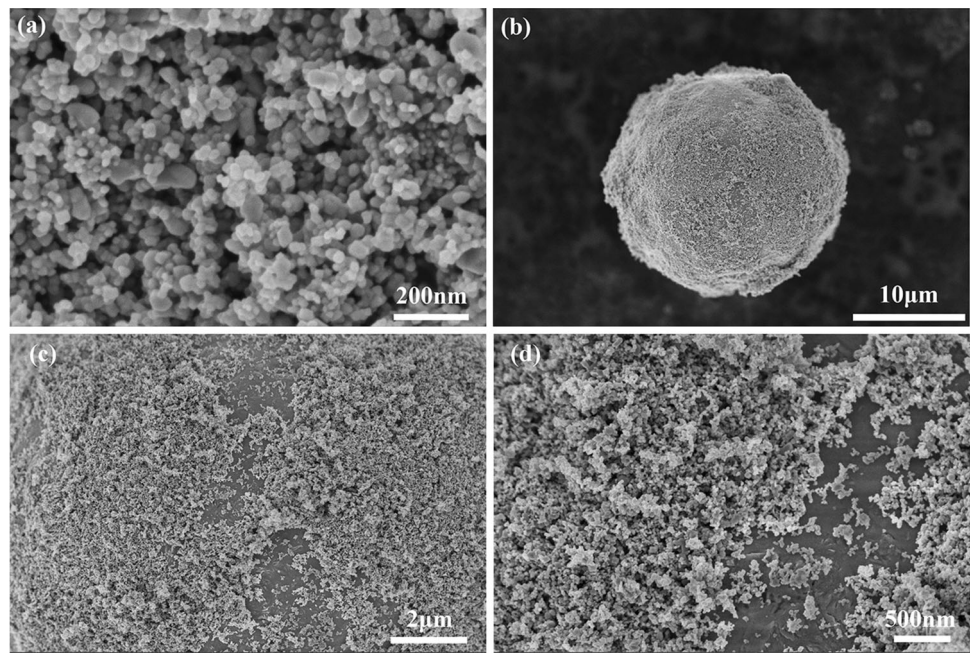


**Fig. 2** XRD patterns of the starting Al-TiO<sub>2</sub> powder feedstock and the cold sprayed Al-TiO<sub>2</sub> coatings (a), and the partially enlarged display of the characteristic peak of titanium dioxide (b)

Further SEM characterization and EDS mapping of the cross sections of the coatings provide clear insight into the formation mechanisms of the nano-TiO<sub>2</sub> particles during the cold spraying (Fig. 5). The light area shown in Fig. 5(a), (b) and (d) is attributed to TiO<sub>2</sub>, and the dark area shown in Fig. 5(a) and (c) is assigned to Al. It is noted that the shape of the agglomerated TiO<sub>2</sub> particles that wrapped Al particle in the starting feedstock has been transformed from spherical to flat contour, which is attributed to the pressing of plastic deformation of Al. Al and TiO<sub>2</sub> particles are staggered in the through-thickness direction, forming a multilayer sandwich structure. The flat Al splats are connected to each other and to the substrate through mechanical interlocking, offering the coating the basic adhesion and cohesion. The evenly distributed TiO<sub>2</sub> layers provide the coating with desired functions. For photocatalytic applications, the cohesion of the nano-TiO<sub>2</sub> particles as attained by anchoring of Al matrix is most likely sufficient.

**Fig. 3** Surface morphologies of the cold sprayed Al-TiO<sub>2</sub> coatings

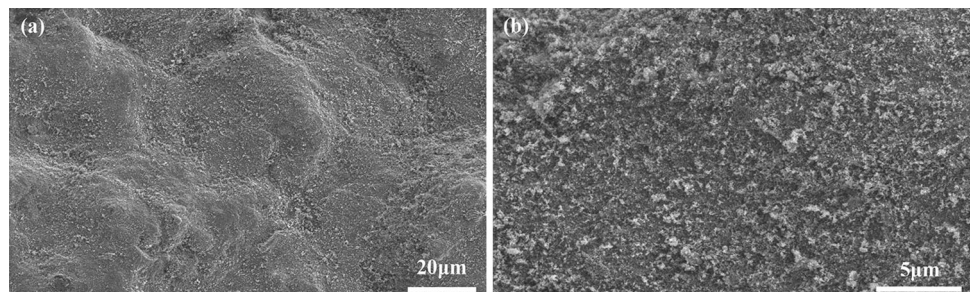


**Fig. 4** Cross-sectional morphology of the cold sprayed Al-TiO<sub>2</sub> composite coatings showing a sandwich-like structure with TiO<sub>2</sub> particles layer being interlocked by Al splats

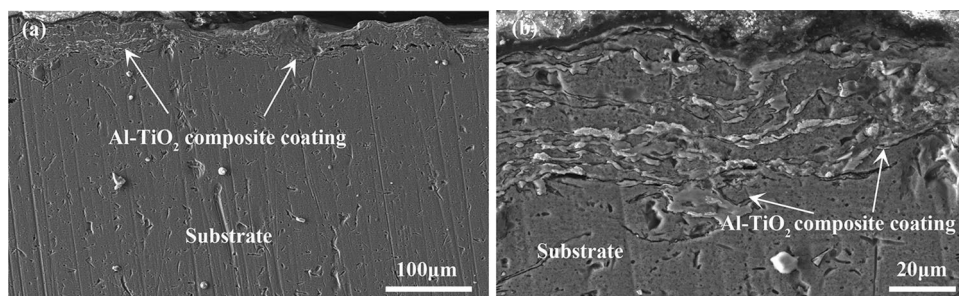


**Fig. 5** Cross-sectional SEM image and EDS mapping of the cold sprayed Al-TiO<sub>2</sub> coatings (element distributions of Ti (b), Al (c) and O (d) were detected from the image (a))

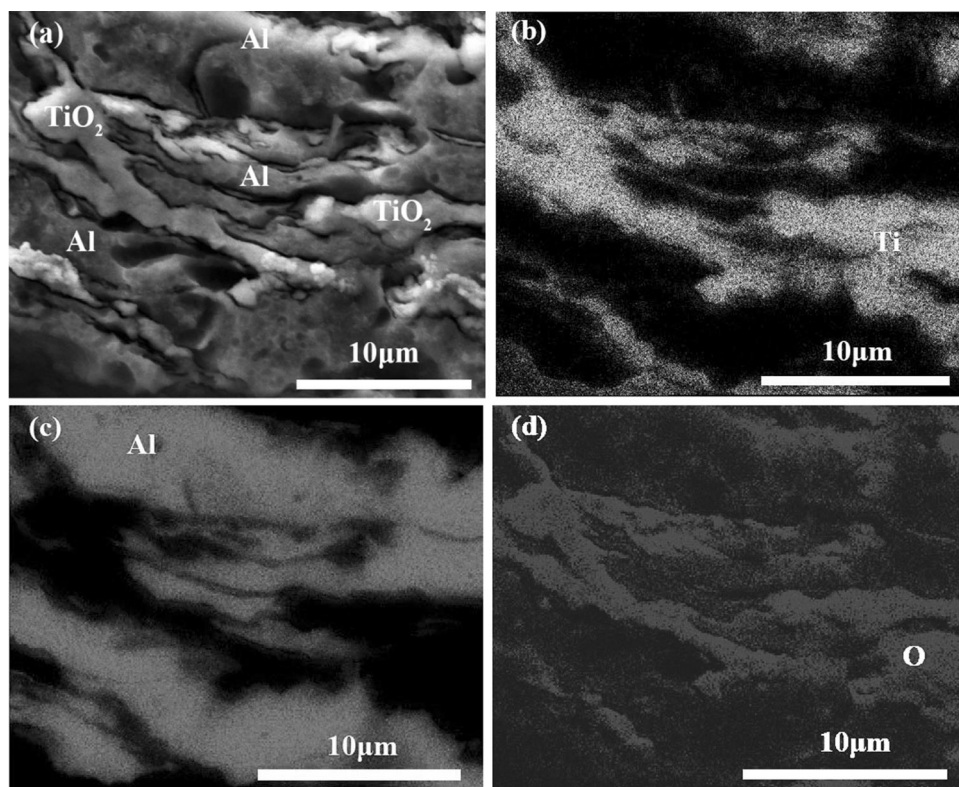
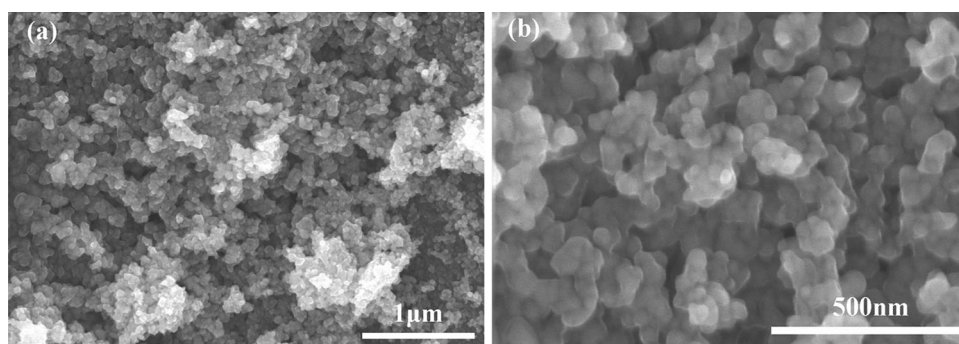


**Fig. 6** SEM morphology of the surface of the initial cold sprayed Al-TiO<sub>2</sub> coatings (a) showing interconnected nano-TiO<sub>2</sub> particles (b)



It is known that photocatalytic coatings play their functions mostly through their surfaces. Topographical views of the Al-TiO<sub>2</sub> composite coatings are shown in Fig. 6. The surface of the coating is covered by a TiO<sub>2</sub> layer with obvious nanostructural features (Fig. 6a), which

would benefit photocatalysis through providing a large number of active sites. The TiO<sub>2</sub> particles are very evenly distributed, and their average particle size is ~30 nm (Fig. 6b), only slightly larger than the starting TiO<sub>2</sub> particles. This implies that during the cold spray processing, the

**Fig. 7** SEM morphology of the surface of the cold sprayed Al-TiO<sub>2</sub> coatings after high-pressure nitrogen blowing showing intact layer of the nano-TiO<sub>2</sub> particles

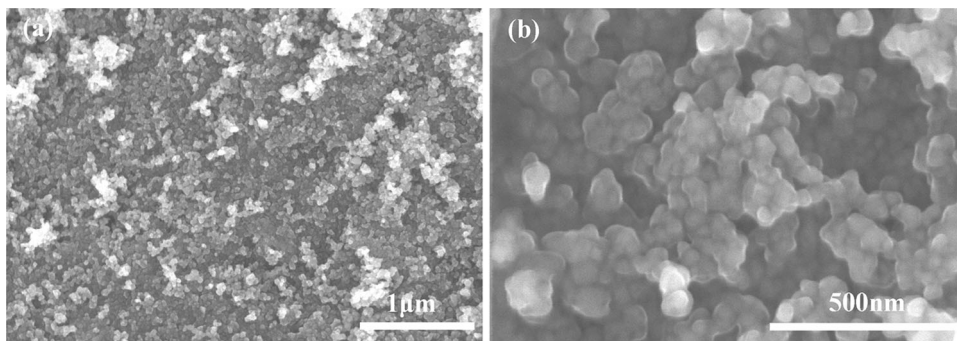


**Fig. 8** SEM morphology of the top layer of the cold sprayed Al-TiO<sub>2</sub> coatings after high-temperature treatment for 1 second showing remarkable grain growth of the TiO<sub>2</sub> articles

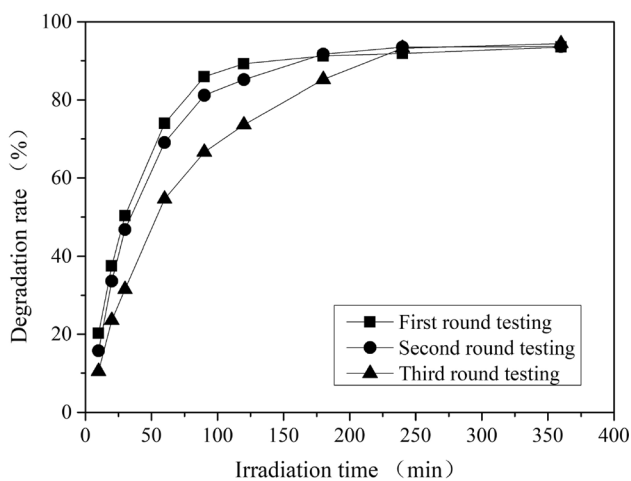
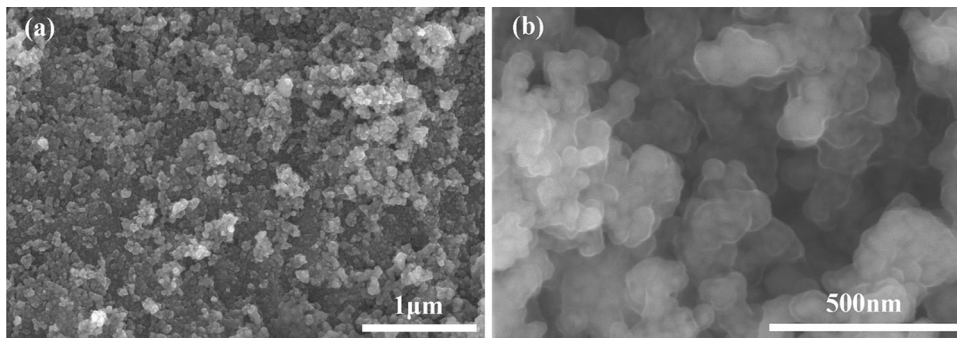


**Fig. 9** Degradation efficiency of MB by the cold sprayed Al-TiO<sub>2</sub> coatings under UV illumination (The examination was repeated for three times for each batch of coating samples)

nanoparticles retained their initial fine size, which is not surprising since the particle heating by the gas plume during the cold spray is limited.

To remove those nano-TiO<sub>2</sub> particles that possibly weakly adhered on the coating surfaces, the Al-TiO<sub>2</sub> coating was blown by high-pressure nitrogen gas on its surface. After the gas blowing, the surface of the coating keeps covered by the TiO<sub>2</sub> layer (Fig. 7a), indicating that the TiO<sub>2</sub> powders indeed adhered to the surface of the coating tightly. In addition, no changes in the topography and the size of the TiO<sub>2</sub> particles are seen (Fig. 7b).

Further surface burning treatment at the temperature above 1500 °C for 1 second using a high-temperature supersonic flame spray gun did not cause loss of the nanostructured TiO<sub>2</sub> layer on the top surface of the coating (Fig. 8). The surface morphology of the treated coating (Fig. 8a and b) is similar to the initial surface (Fig. 6). It therefore suggests that the cold sprayed Al-TiO<sub>2</sub> composite coating has a stable titania top layer, which consists of nano-TiO<sub>2</sub> particles with firm adhesion on the Al matrix. Furthermore, however, sintering of adjacent TiO<sub>2</sub> particles and growth of particle size are observed (Fig. 8b), the size of the TiO<sub>2</sub> particles is up to 75 nm, being significantly larger than the original TiO<sub>2</sub> particles in the starting feedstock powder. This phenomenon nevertheless indicates that the aggregation of TiO<sub>2</sub> particles and following grain growth occurred during the short-term high-temperature treatment. This on the other hand indicates the poor dimensional thermal stability of the nano-TiO<sub>2</sub> particles. Cold spray processing route showed great potential for depositing nanosized temperature-sensitive materials for retaining their original physicochemical properties.

Photocatalytic testing showed promising activity of the cold sprayed coatings (Fig. 9). It has been clear that nanotitania with anatase structure has desired photocatalytic performances (Ref 27, 32). To reveal the repeatable photocatalytic functions of the Al-TiO<sub>2</sub> coatings, examination of the UV photocatalytic degradation of MB was carried out for three times for each coating sample. The results show that the 1.5-hour degradation rates of the first, the

second and the third round testing are 85.9%, 81.2% and 66.7%, respectively, and the 3-hour degradation rates of the first, the second and the third round testing are 91.2%, 91.7%, and 85.2%, respectively. The 6-hour degradation rates of the first, the second and the third round testing are 93.5%, 93.6% and 94.4%, respectively. After 3 hours of UV light irradiation, the degradation rates of the coatings are above 85% even after the third time testing for the same coating samples. The 6-hour degradation rates are still above 93%. These results suggest excellent repeatable degradation performances of the cold sprayed Al-TiO<sub>2</sub> coatings. It was also noted that the MB degradation rate of the coatings for the 4-hour third time testing also reached 93.2%, indicating good reusability of the Al-TiO<sub>2</sub> coatings for photocatalytic applications. The recycling performances of the coatings as revealed by the MB degradation measurement were further explained by the intact topographical morphologies of the coatings after the photocatalytic testing (images not shown). It was noted that after 6 h photocatalytic testing in MB-containing solution, the surfaces of the coatings kept intact. The nano-TiO<sub>2</sub> top layer retained the initial sizes of the nano-TiO<sub>2</sub> particles.

## Conclusions

In this work, Al-TiO<sub>2</sub> composite powder with spherical Al particle being wrapped by a thick layer of nano-TiO<sub>2</sub> particles was designed as the powder feedstock to make nano-TiO<sub>2</sub>-containing coatings by cold spraying. Sandwich-like structure was constructed for the cold sprayed Al-TiO<sub>2</sub> coatings, and the thin layers of nano-TiO<sub>2</sub> particles were mechanically interlocked by the Al matrix in the coatings. A strongly adhered layer comprising nano-TiO<sub>2</sub> particles exists on the top surface of the coatings and keeps intact after photocatalytic testing carried out in aqueous solutions. Excellent photocatalytic activities and good reusability of the cold sprayed Al-TiO<sub>2</sub> coatings were revealed. The results would give insight into structure design and cold spray coating fabrication of temperature-sensitive functional nanomaterials for a variety of applications.

**Acknowledgements** This research was supported by K.C. Wong Education Foundation (Grant # GJTD-2019-13) and Jiangxi Province Key Research and Development Projects of China (Grant # 20192BBE50033, 20202BBEL53031 and 20192BBHL80010).

## References

1. A. Fujishima and K. Honda, Electrochemical Photolysis of Water at a Semiconductor Electrode, *Nature*, 1972, **238**, p 37–38.
2. M. Zhai, Y. Liu, J. Huang, Y. Wang, K. Chen, Y. Fu and H. Li, Efficient Suspension Plasma Spray Fabrication of Black Titanium Dioxide Coatings with Visible Light Absorption Performances, *Ceram. Int.*, 2019, **45**, p 930–935.
3. M. Bozorgtabar, M. Rahimipour and M. Salehi, Novel Photocatalytic TiO<sub>2</sub> Coatings Produced by HVOF Thermal Spraying Process, *Mater. Lett.*, 2010, **64**(10), p 1173–1175.
4. M. Winnicki, A. Baszczuk, M. Jasiorski, B. Borak and A. Malachowska, Preliminary Studies of TiO<sub>2</sub> Nanopowder Deposition onto Metallic Substrate by Low Pressure Cold Spraying, *Surf. Coat. Technol.*, 2019, **371**, p 194–202.
5. C. Orge, J.L. Faria and M.F.R. Pereira, Photocatalytic Ozonation of Aniline with TiO<sub>2</sub>-Carbon Composite Materials, *J. Environ. Manag.*, 2017, **195**, p 208–215.
6. A. Mishra, A. Mehta and S. Basu, Clay Supported TiO<sub>2</sub> Nanoparticles for Photocatalytic Degradation of Environmental Pollutants: A Review, *J. Environ. Chem. Eng.*, 2018, **6**(5), p 6088–6107.
7. V.G. Parale, T. Kim, V.D. Phadtare, H.M. Yadav and H. Park, Enhanced Photocatalytic Activity of a Mesoporous TiO<sub>2</sub> Aerogel Decorated onto Three-Dimensional Carbon Foam, *J. Mol. Liq.*, 2019, **277**, p 424–433.
8. L. Lu, R. Shan, Y. Shi, S. Wang and H. Yuan, A novel TiO<sub>2</sub>/Biochar Composite Catalysts for Photocatalytic Degradation of Methyl Orange, *Chemosphere*, 2019, **222**, p 391–398.
9. A. Baszczuk, M. Jasiorski, B. Borak and J. Wodka, Insights into the Multistep Transformation of Titanate Nanotubes into Nanowires and Nanoribbons, *Mater. Sci. Poland*, 2016, **34**(4), p 691–702.
10. Y. Tsuge, J. Kim, Y. Sone, O. Kuwaki and S. Shiratori, Fabrication of Transparent TiO<sub>2</sub> Film with High Adhesion by Using Self-Assembly Methods: Application to Super-Hydrophilic Film, *Thin Solid Films*, 2008, **516**(9), p 2463–2468.
11. H. Attouche, S. Rahmane, S. Hettal and N. Kouidri, Precursor Nature and Molarities Effect on the Optical, Structural, Morphological, and Electrical Properties of TiO<sub>2</sub> Thin Films Deposited by Spray Pyrolysis, *Optik*, 2020, **203**, p 163985.
12. T. Vladkova, O. Angelov, D.S. Stoyanova, D.N. Gospodinova, L. Gomes, A. Soares, F. Mergulhao and I. Ivanovac, Magnetron Co-Sputtered TiO<sub>2</sub>/SiO<sub>2</sub>/Ag Nanocomposite Thin Coatings Inhibiting Bacterial Adhesion and Biofilm Formation, *Surf. Coat. Technol.*, 2020, **384**, p 125322.
13. B. Jeffery, M. Pepler, R.S. Lima and A. McDonald, Bactericidal Effects of HVOF-Sprayed Nanostructured TiO<sub>2</sub> on *Pseudomonas Aeruginosa*, *J. Therm. Spray Technol.*, 2010, **19**, p 344–349.
14. X. He, K. Ren, Y. Liu, J. Huang and H. Li, Hollow Plasma-Sprayed Spherical Nanostructured Titania Feedstock for Photocatalytic Applications, *J. Therm. Spray Technol.*, 2018, **27**, p 1532–1541.
15. R. Lima and B.R. Marple, Thermal Spray Coatings Engineered from Nanostructured Ceramic Agglomerated Powders for Structural, Thermal Barrier and Biomedical Applications: A Review, *J. Therm. Spray Technol.*, 2007, **16**, p 40–63.
16. N. George, M. Mahon and A. McDonald, Bactericidal Performance of Flame-Sprayed Nanostructured Titania-Copper Composite Coatings, *J. Therm. Spray Technol.*, 2010, **19**, p 1042–1053.
17. Y. Fu, Y. Liu and H. Li, Onion-Like Carbon Modified TiO<sub>2</sub> Coating by Suspension Plasma Spray and Enhanced Photocatalytic Performances, *J. Nanopart. Res.*, 2019, **21**, p 182.
18. J.H. Leal, Y. Cantu, D.F. Gonzalez and J.G. Parsons, Brookite and Anatase Nanomaterial Polymorphs of TiO<sub>2</sub> Synthesized from TiCl<sub>3</sub>, *Inorg. Chem. Commun.*, 2017, **84**, p 28–32.
19. A. Viscusi, M. Durante, A. Astarita, L. Boccarusso, L. Carrino and A.S. Perna, Experimental Evaluation of Metallic Coating on Polymer by Cold Spray, *Procedia Manuf.*, 2020, **47**, p 761–765.

20. M. Gardon, C. Fernández-Rodríguez, D. Garzón Sousa, D.J.M. Doña-Rodríguez, S. Dosta, I.G. Cano and J.M. Guilemany, Photocatalytic Activity of Nanostructured Anatase Coatings Obtained by Cold Gas Spray, *J. Therm. Spray Technol.*, 2014, **23**, p 1135–1141.
21. J. Freitag and D.W. Bahnemann, Evaluation of the Photocatalytic (Visible-Light) Activity of Cold Gas Sprayed TiO<sub>2</sub> Layers on Metal Sheets, *Phys. Status Solid A.*, 2014, **8**(6), p 596–599.
22. I. Herrmann-Geppert, P. Bogdanoff, T. Emmeler, Th. Dittrich, J. Radnik, T. Klassen, H. Gutzmann and M. Schieda, Cold Gas Spraying-A Promising Technique for Photoelectrodes: The Example TiO<sub>2</sub>, *Catal. Today*, 2016, **260**, p 140–147.
23. C.J. Li, G.J. Yang, W.Y. Li, X.C. Huang, and A. Ohmori, Formation of TiO<sub>2</sub> Photocatalyst through Cold Spraying, in *Proceedings of Thermal Spray 2004, Advances in Technology and Application*, Osaka, Japan, p 315-319 (2004)
24. I. Burlacov, J. Jirkovsky, L. Kavan, R. Ballhorn and R.B. Heilmann, Cold Gas Dynamic Spraying (CGDS) of TiO<sub>2</sub> (anatase) Powders onto Poly(Sulfone) Substrates: Microstructural Characterisation and Photocatalytic Efficiency, *J. Photochem. Photobiol. A*, 2007, **187**(2–3), p 285–292.
25. I. Herrmann-Geppert, P. Bogdanoff, H. Gutzmann, T. Dittrich, T. Emmeler, R. Just, M. Schieda, F. Gärtner and T. Klassen, Cold Gas Sprayed TiO<sub>2</sub>-Based Electrodes for the Photo-Induced Water Oxidation, *ECS Trans.*, 2014, **58**(30), p 21–30.
26. J.O. Kliemann, H. Gutzmann, F. Gärtner, H. Hübner, C. Borchers and T. Klassen, Formation of Cold-Sprayed Ceramic Titanium Dioxide Layers on Metal Surfaces, *J. Therm. Spray Technol.*, 2011, **20**(1–2), p 292–298.
27. M. Yamada, Y. Kandori, K. Sato and M. Fukumoto, Fabrication of Titanium Dioxide Photocatalyst Coatings by Cold Spray, *J. Solid Mech. Mater. Eng.*, 2009, **3**(2), p 210–216.
28. Sh.Q. Fan, Ch.J. Li, Ch.X. Li, G.J. Liu, G.J. Yang and L.Z. Zhang, Preliminary Study of Performance of Dye-Sensitized Solar Cell of Nano-TiO<sub>2</sub> Coating Deposited by Vacuum Cold Spraying, *Mater. Trans.*, 2006, **47**(7), p 1703–1709.
29. A.A. Pustovalova, V.F. Pichugin, N.M. Ivanova and M. Bruns, Structural Features of N-Containing Titanium Dioxide Thin Films Deposited by Magnetron Sputtering, *Thin Solid Films*, 2017, **627**, p 9–16.
30. L. Huang, J. Xu, X. Sun, Ch. Li, R. Xu, Y. Du, J. Ni, H. Cai, J. Li, Z. Hu and J. Zhang, Low-Temperature Photochemical Activation of Sol-Gel Titanium Dioxide Films for Efficient Planar Heterojunction Perovskite Solar Cells, *J. Alloys Compd.*, 2018, **735**, p 224–233.
31. M. Ratova, R. Klaysri, P. Praserttham and P.J. Kelly, Visible Light Active Photocatalytic C-Doped Titanium Dioxide Films Deposited via Reactive Pulsed DC Magnetron Co-Sputtering: Properties and Photocatalytic Activity, *Vacuum*, 2018, **149**, p 214–224.
32. Y. Liu, J. Huang, X. Feng and H. Li, Thermal-Sprayed Photocatalytic Coatings for Biocidal Applications: A Review, *J. Therm. Spray Technol.*, 2020 <https://doi.org/10.1007/s11666-020-01118-2>

**Publisher's Note** Springer Nature remains neutral with regard to jurisdictional claims in published maps and institutional affiliations.